Accepted Manuscript

Transcriptome sequencing and metabolic pathways of astaxanthin accumulated in *Haematococcus pluvialis* mutant under 15% CO_2

Jun Cheng, Ke Li, Yanxia Zhu, Weijuan Yang, Junhu Zhou, Kefa Cen

PII: S0960-8524(16)31762-X
DOI: http://dx.doi.org/10.1016/j.biortech.2016.12.084
Reference: BITE 17460

To appear in: *Bioresource Technology*

Received Date: 2 November 2016
Revised Date: 8 December 2016
Accepted Date: 22 December 2016

Please cite this article as: Cheng, J., Li, K., Zhu, Y., Yang, W., Zhou, J., Cen, K., Transcriptome sequencing and metabolic pathways of astaxanthin accumulated in *Haematococcus pluvialis* mutant under 15% CO_2, *Bioresource Technology* (2016), doi: http://dx.doi.org/10.1016/j.biortech.2016.12.084

This is a PDF file of an unedited manuscript that has been accepted for publication. As a service to our customers we are providing this early version of the manuscript. The manuscript will undergo copyediting, typesetting, and review of the resulting proof before it is published in its final form. Please note that during the production process errors may be discovered which could affect the content, and all legal disclaimers that apply to the journal pertain.

ACCEPTED MANUSCRIPT

Transcriptome sequencing and metabolic pathways of astaxanthin accumulated in *Haematococcus pluvialis* mutant under 15% CO_2

Jun Cheng*[a], Ke Li[a], Yanxia Zhu[a], Weijuan Yang[a], Junhu Zhou[a], Kefa Cen[a]

State Key Laboratory of Clean Energy Utilization, Zhejiang University, Hangzhou 310027, China

Abstract:

Transcriptome sequencing and annotation was performed on *Haematococcus pluvialis* mutant red cells induced with high light under 15% CO_2 to demonstrate why astaxanthin yield of the mutant was 1.7 times higher than that of a wild strain. It was found that 56% of 1,947 differentially expressed genes were upregulated in mutant cells. Most significant differences were found in unigenes related to photosynthesis, carotenoid biosynthesis and fatty acid biosynthesis pathways. The pyruvate kinase increased by 3.5-fold in mutant cells. Thus, more pyruvate, which was beneficial to carotenoids and fatty acid biosynthesis, was generated. Phytoene synthase, zeta-carotene desaturase, lycopene beta-cyclase involved in β-carotene biosynthesis in mutant cells were upregulated by 10.4-, 4.4-, and 5.8-fold, respectively. Beta-carotene 3-hydroxylase catalyzing conversion of β-carotene into astaxanthin was upregulated by 18.4-fold. The fatty acid biosynthesis was promoted because of the upregulation of acetyl-CoA synthetase and acetyl-CoA carboxylase, thus increasing astaxanthin esterification and accumulation in mutant cells.

Keywords: *Haematococcus pluvialis*, astaxanthin, mutant cells, transcriptome sequencing, metabolic pathways

1. Introduction

Microalgae production is widely considered for removing CO_2 from the flue gas of coal-fired power plants, and its biomass can be a feedstock for biodiesel and various high valued products, such as astaxanthin (Cheng et al., 2016a; Williams and Laurens, 2010; Zheng et al., 2016). *Haematococcus pluvialis* with the highest astaxanthin content in nature is the only commercialized microalgae in astaxanthin production. Astaxanthin accumulation is generally assumed to be a survival strategy adopted by *H. pluvialis* grown in stressful environments, which is important in energy and carbon storage, and in quenching the reactive oxygen species generated during stress response (Lemoine and Schoefs, 2010; Li et al., 2008; Yuan et al., 2011). However, the mechanism underlying the enhanced astaxanthin yield of *H. pluvialis* mutant under high concentration of CO_2 has not been fully documented.

Transcriptome sequencing is an efficient approach for obtaining microalgae functional genomics information. This method has identified the key pathways and important genes for biofuel production, molecular changes promoting or accompanying triacylglycerol accumulation, and molecular mechanism of carbon sequestration(Rismani-Yazdi et al., 2011; Cheng et al., 2014; Fan et al., 2016; Miller et al., 2010). Many studies have also discussed the gene transcript and metabolic changes of *H. pluvialis* responding to various stress (e.g., light, salinity, temperature, hormone, iron and inorganic carbon) (Gao et al., 2015; Hong et al., 2015; Li et al., 2010; Wen et al., 2015). Protein-encoding genes involved in the

ACCEPTED MANUSCRIPT

metabolism of carbohydrate, energy and amino acids were increased with hormone induction (Gao et al., 2015). The non-mevalonate pathway mediating the synthesis of isopentenyl diphosphate was upregulated, and de novo fatty acid biosynthesis and the TAG assembly pathways were elevated under high light (Gwak et al., 2014). However, astaxanthin accumulation is also correlated to many other metabolite pathways such as fatty acid and triacylglycerol biosynthesis (Solovchenko, 2015). Further studies should be made on genomics, proteomics, and metabolomics with regard to the induction and regulation of astaxanthin biosynthesis.

Our previous works showed that high CO_2 concentration can enhance the growth rate and astaxanthin yield of *H. pluvialis* mutant. The astaxanthin content of the mutant under 15% CO_2 was 40% higher than that of the wild cells under air (0.04% CO_2) under high light (Cheng et al., 2016a, b). So, here we compared the wild cells incubated under air and mutant cells incubated under 15%CO_2 at gene levels to inspect genes that encode enzymes involved in astaxanthin accumulation and to discuss the mechanism underlying the enhancement of astaxanthin content in *H. pluvialis* mutant under 15% CO_2. 15% CO_2 was employed because it is an average concentration of CO_2 from flue gas in most coal-fired power plants whose application in industry may increase the astaxanthin yield while decrease the costs. Results demonstrated that the transcript levels of astaxanthin genes were enhanced by 15% CO_2. The active pyruvate metabolism provided more precursor to astaxanthin, and the enhanced fatty acid biosynthesis pathway conferred a high capacity of astaxanthin deposit in lipid droplets.

2. Materials and Methods

2.1 Culturing and harvesting of *H. pluvialis*

The wild *H. pluvialis* strain used in this study was purchased from the Freshwater Algae Culture Collection of Hydrobiology, Chinese Academy of Sciences. The *H. pluvialis* mutant was isolated from ^{60}Co-γ irradiated strains and domesticated with 15% CO_2 (Cheng et al., 2016a). Microalgae cells were cultured in Bold's Basal Medium, and aerated continuously with air for the wild strain and 15% CO_2 (v/v, CO_2/N_2) for the mutant. Vegetative cultivation was performed under 65 μmol photons m^{-2} s^{-1} of continuous light with 120mL min^{-1} aeration rate. Encystment induction was performed under 250 μmol photons m^{-2} s^{-1} of continuous light with 240 mL min^{-1} aeration rate. Samples were collected through centrifugation after 18 h of high-light induction, maintained in liquid-nitrogen for 10 min, and then stored at - 79 °C until further analysis.

2.2 Growth and astaxanthin analyses

The biomass dry weight was measured gravimetrically. The specific growth rate (μ) was calculated as follows (Tang et al., 2011):

$$\mu = (\ln M_1 - \ln M_0) / (t_1 - t_0), \quad (1)$$

ACCEPTED MANUSCRIPT

where M_1 and M_0 are the dry weight at time t_1 and t_0, respectively .

Astaxanthin yield was measured via spectrophotometric method (Boussiba et al., 1992). The harvested cells were first treated with 5% (w/v) KOH in 30% (v/v) methanol to eliminate the chlorophyll. The supernatant was discarded, and the remaining pellet was extracted with DMSO to recover the astaxanthin. The extraction procedure was repeated until the cell debris was nearly colourless. The absorbance of the combined extracts was determined at 490 nm, and the per unit volume astaxanthin concentration (c) was calculated as follows:

$$c\ (\text{mg/L}) = 4.5 \times A_{490} \times V_a / V_b, \quad (2)$$

where V_a and V_b are the volume of extracts and culture sample, respectively, and A_{490} is the absorbance of the extracts at 490 nm.

2.3 RNA extraction and cDNA library construction

Total RNA was extracted using Kits (mirVana™ miRNA ISOlation Kit，Ambion-1561) in accordance with the manufacturer's protocol. RNA integrity was evaluated using the Agilent 2100 Bioanalyzer (Agilent Technologies, Santa Clara, CA, USA). Samples with RNA integrity number ≥7 were subjected to subsequent analysis. Libraries were constructed using the TruSeq Stranded mRNA LT Sample Prep Kit (Illumina, San Diego, CA, USA) in accordance with the manufacturer's instructions. Purification was conducted using AMPure XP beads (Beckman Coulter, Brea, A63881). The purified samples were amplified via PCR reaction. The libraries were validated using Agilent 2100 Bioanalyzer, and the qualified libraries were sequenced on the Illumina sequencing platform (HiSeqTM 2500). Finally, 150 bp /125 bp paired-end reads were generated.

2.4 Sequence assembly and annotation

Raw reads were processed using NGS QC Toolkit. Reads containing ploy-N and the low-quality reads were removed to obtain clean reads, which were then mapped to the reference genome using Tophat (http://tophat.cbcb.umd.edu/). The reads were reassembled using the Tophat-Cufflinks platform. Gene structure extension and novel transcript identification were performed by comparing reference genome and known annotated genes using Cuffcompare software. Following the assembly, unigenes were compared with the non-redundant database using Blastx, with a cut-off E-value of $< 10^{-5}$. Gene Ontology (GO) annotations and corresponding enzyme commission numbers (ECs) of the sequences were obtained by Blast2Go. Kyoto Encyclopedia of Genes and Genomes (KEGG) mapping was used to characterize the metabolic pathways. Unigenes with corresponding Blast2GO-obtained ECs were mapped to the KEGG metabolic pathway database, and submitted to the KEGG Automatic Annotation Server (KAAS). KAAS annotates every submitted unigene with KEGG orthology (KO) identifiers, which represent an ortholog group of genes directly linked to an object in the KEGG pathway and BRITE functional hierarchy, and

ACCEPTED MANUSCRIPT

incorporating different types of relationships that exist in biological systems. The FPKM value of each gene was calculated using Cufflinks (version 1.3.0), and the read counts of each gene were obtained by HTSeq package in 2010. Differentially expressed genes (DEGs) were identified using the DESeq (2012) R package, functions estimateSizeFactors and nbinomTest. $P < 0.05$ was set as the threshold to indicate significant differential expression. Hierarchical cluster analysis of DEGs was performed to explore gene expression patterns. GO and KEGG pathway enrichment analyses of DEGs were performed using R based on hypergeometric distribution.

3. Results and discussion

3.1 Growth and gene expression comparison

The astaxanthin yield of *H. pluvialis* mutant under 15%CO_2 increased by 2.7 times as that of the wild strain under air (Fig.1b). The biomass of the mutant was increased by 2 times as the initial in 12h (Fig.1a), while the astaxanthin biosynthesis was not as fast as carbohydrate, so the astaxanthin content was decreased in the 12h. After 36h, the biomass increase was slowed down, and the astaxanthin content increased. Studies shows that 80% of photosynthetic carbon is directed toward sugars, and then converted into other metabolites (Melis, 2012). The initial storage of carbohydrate under 15% CO_2 provides more feedstock and energy, while the enhanced astaxanthin biosynthesis pathway make a good use of them to increase astaxanthin production. De novo assembly of transcriptomes revealed the genomic and metabolic features of the mutant under high CO_2. Sequencing of cDNA libraries of the mutant and the wild strain generated a total of 18.2 million and 18.5 million raw reads, respectively. According to the standard of $p < 0.05$, DEGs including 1,097 upregulated and 850 downregulated unigenes were identified (Fig.2a). The upregulated unigenes were further annotated with GO terms (Fig.2b), and the identified major subcategories were photosynthesis, fatty acid biosynthesis, carotenoid biosynthesis, light-harvesting complex, PSII, chlorophyll binding and oxidoreductase activity. These explain the surge of biomass and astaxanthin yield of the mutant under 15%CO_2.

3.2 Transcriptome and pathway analysis involved in pyruvate metabolism

Most microalgae photosynthetic carbon is directed toward sugars, and then converted into lipid (Melis, 2012; Recht et al., 2012). Pyruvate metabolism plays a major role in shuttling carbon toward lipid synthesis (Equation 3) (Levitan et al., 2015), and the product-to-biomass carbon-partitioning ratio affects the final yield. Secondary carotenoids synthesis also shows a positive correlation with pyruvate (Chen et al., 2009; Kobayashi et al., 1991). The conversion of phosphoenol pyruvate into pyruvate was significantly enhanced by the 3.5-fold upregulation of PK (Table 1), thus promoting the whole pyruvate metabolism of the mutant under 15% CO_2. Pyruvate may interact with 3-phosphoglycerol aldehyde of mesophyll, yielding the substrate for isopentenyl pyrophosphate (IPP) production (Saakov, 2005). The

ACCEPTED MANUSCRIPT

increased pyruvate significantly upregulated the geranyl diphosphate synthase, which catalyzed the synthesis of Geranyl-PP (see metabolic pathway in Electronic Supplementary Information), thus providing more carotenoid precursor and enhancing the carotenoid biosynthesis pathways. The PDHB and ACSS were upregulated 3.7- and 2.9-fold, respectively, which could possibly result in an increase of acetyl-coA (Fig.3). The increasing acetyl-coA stimulates lipid synthesis, which is the main depot for astaxanthin. PC, which converts pyruvate into oxaloacetate, was upregulated by 7.4-fold. NADP-ME, which supplies both carbon and reducing equivalents in the form of NADPH for de novo fatty acid production, was upregulated by 8.9-fold (Shtaida et al., 2015).

$$\text{glucose} + 2NAD^+ + 2ADP + 2Pi = 2\,(\text{pyruvate} + ATP + NADH + H^+), \quad (3)$$

3.3 Transcriptome and pathway analysis involved in astaxanthin biosynthesis

Gamma irradiation and oxygen radicals generated by water radiolysis increase the astaxanthin yield by inducing chromosomal rearrangement (Najafi et al., 2013). The increase of inorganic carbon also upregulates the carotenoid biosynthesis related genes (Wen et al., 2015). As for primary carotenoid biosynthesis, the universal isoprenoid precursor IPP and its allylic isomer dimethyl allyl pyrophosphate are synthesized along the non-mevalonate pathway (Lemoine and Schoefs, 2010), and their condensation reaction between IPP and DMAPP yields geranylgeranyl pyrophosphate (GGPP). The condensation of two GGPP molecules into phytoene is catalyzed by phytoene synthase, which was upregulated by 10.4-fold under 15%CO_2 (Fig. 4). The conversion of phytoene into β-carotene is successively catalyzed by PDS, ZDS and lcyB, which were upregulated by 3.2-, 4.4-, and 5.8-fold, respectively under 15%CO_2. The reactions catalyzed by PDS are among the rate-limiting steps of the pathway, and the PDS gene upregulation may confer a higher astaxanthin synthesis capacity (Li et al., 2010). Astaxanthin is produced at the expense of β-carotene in two pathways, i.e., oxidation and hydroxylation of β-carotene (Kobayashi, 2003). The later was enhanced because of 17-fold upregulation of crtZ under 15%CO_2 (Equation 4), which may be attributed to the increase of NADH and H^+ generated via the glycolysis pathway (Equation 3).

$$\beta\text{-carotene} + 2\,NADH + 2\,H^+ + 2\,O_2 = \text{zeaxanthin} + 2\,NAD^+ + 2\,H_2O, \quad (4)$$

3.4 Transcriptome and pathway analysis involved in fatty acid biosynthesis

Astaxanthin in *H. pluvialis* is linearly correlated with accumulation of fatty acid (Zhekisheva et al., 2002). The increased neutral lipids are hypothesized to serve as a matrix for solubilizing astaxanthin esters (Saha et al., 2013). Astaxanthin cannot accumulate in appreciable amounts within the thylakoid membranes or in free form within the hydrophilic environment of the cytoplasm. Massive astaxanthin is esterified in the endoplasmic reticulum, and deposits in cytoplasmic lipid droplets, thus avoiding the feedback inhibitor of carotenoids biosynthesis. Lipid droplets may also protect hydrophobic β-carotene ketolase from the protease attack, which may explain continued enzyme activation when mRNA content is decreased

ACCEPTED MANUSCRIPT

(Solovchenko, 2015). The formation of lipid droplets is key factor that drives and limits astaxanthin accumulation. Under 15%CO_2, a high amount of carbon flows from pyruvate to acetyl-CoA, and cellular HCO_3^- accumulation was greater than that under air (Gross, 2000) (Equation 4). Acetyl-CoA carboxylase was upregulated by 3.6-fold, thereby enhancing the carboxylation of acetyl-CoA to malonyl-CoA. FabD was upregulated by 6.7-fold, thus enhancing the formation of malonyl-ACP from malonyl-CoA. FabH, which catalyzes the condensation between acetyl-CoA and malonyl-ACP to form acetoacetyl-ACP, was upregulated by 3.1-fold (Fig. 5). The acyl chain elongation begins with the condensation reaction between malonyl-ACP and acyl-ACP, which is generated from acetoacetyl-ACP. The acyl chain is lengthened by two carbon atoms in each turn until palmitoyl- ACP is formed (Sanchez and Harwood, 2002). Then fatty acid with longer chains and unsaturated fatty acid were formed via sequent decarbonation and desaturation.

ATP + acetyl-CoA + HCO_3^- = ADP + phosphate + malonyl-CoA (4)

4. Conclusions

Transcriptome sequencing analysis indicated that ^{60}Co- γ ray mutagenesis and 15% CO_2 domestication enhanced astaxanthin biosynthesis in *H. pluvialis*. The enhanced pyruvate metabolic pathway provided astaxanthin biosynthesis with primary metabolites as feedstock. The upregulation of genes involved in β-carotene biosynthesis (e.g., PSY, ZDS and lcyB) and β-carotene conversion (e.g., crtZ) accelerated astaxanthin biosynthesis. The upregulation of acetyl-CoA synthetase and acetyl-CoA carboxylase enhanced fatty acid biosynthesis, thus promoting astaxanthin esterification and deposition. For further studies, investigation of time-dependent transcriptomic analyses is needed to observe the dynamic changes in astaxanthin biosynthesis pathways in response to high CO_2 concentration.

Acknowledgements

This work was supported by National Natural Science Foundation-China (51476141), National key research and development program-China (2016YFB0601003), Zhejiang Provincial Natural Science Foundation - China (LR14E060002).

References

[1] Boussiba, S., Fan, L., Vonshak, A., 1992. Enhancement and determination of astaxanthin accumulation in green-alga *Haematococcus pluvialis*. *Method Enzymol.*. 213, 386-391.

[2] Chen, T., Wei, D., Chen, G., Wang, Y., Chen, F., 2009. Employment of organic acids to enhance astaxanthin formation in heterotrophic Chlorella zofingiensis. *J. Food Process Pres.*. 33, 271-284.

[3] Cheng, J., Li, K., Yang, Z., Lu, H., Zhou, J., Cen, K., 2016a. Gradient domestication of *Haematococcus*

ACCEPTED MANUSCRIPT

pluvialis mutant with 15% CO_2 to promote biomass growth and astaxanthin yield. *Bioresource Technol.*. 216, 340-344.

[4] Cheng, J., Li, K., Yang, Z., Zhou, J., Cen, K., 2016b. Enhancing the growth rate and astaxanthin yield of *Haematococcus pluvialis* by nuclear irradiation and high concentration of carbon dioxide stress. *Bioresource Technol.*.204, 49-54.

[5] Cheng, R., Feng, J., Zhang, B., Huang, Y., Cheng, J., Zhang, C., 2014. Transcriptome and gene expression analysis of an oleaginous diatom under different salinity conditions. *Bioenerg. Res.*. 7, 192-205.

[6] Fan, J., Xu, H., Li, Y., 2016. Transcriptome-based global analysis of gene expression in response to carbon dioxide deprivation in the green algae *Chlorella pyrenoidosa*. *Algal Res.*. 16, 12-19.

[7] Gao, Z., Li, Y., Wu, G., Li, G., Sun, H., Deng, S., Shen, Y., Chen, G., Zhang, R., Meng, C., Zhang, X., 2015. Transcriptome analysis in *Haematococcus pluvialis*: astaxanthin induction by salicylic acid (SA) and jasmonic acid (JA). *PLoS One*. 10.

[8] Gao, Z., Meng, C., Chen, Y.C., Ahmed, F., Mangott, A., Schenk, P.M., Li, Y., 2015. Comparison of astaxanthin accumulation and biosynthesis gene expression of three *Haematococcus pluvialis* strains upon salinity stress. *J. Appl. Phycol.*. 27, 1853-1860.

[9] Gross, W., 2000. Ecophysiology of algae living in highly acidic environments. *Hydrobiologia*, 433, 31-37.

[10] Gwak, Y., Hwang, Y., Wang, B., Kim, M., Jeong, J., Lee, C., Hu, Q., Han, D., Jin, E., 2014. Comparative analyses of lipidomes and transcriptomes reveal a concerted action of multiple defensive systems against photooxidative stress in *Haematococcus pluvialis*. *J. Exp. Bot.*. 65, 4317-4334.

[11] Hong, M., Hwang, S.K., Chang, W.S., Kim, B.W., Lee, J., Sim, S.J., 2015. Enhanced autotrophic astaxanthin production from *Haematococcus pluvialis* under high temperature via heat stress-driven Haber-Weiss reaction. *Appl. Microbiol. Biot.*. 99, 5203-5215.

[12] Kobayashi, M., 2003. Astaxanthin biosynthesis enhanced by reactive oxygen species in the green alga Haematococcus pluvialis. *Biotechnol. Bioproc. E.*. 8, 322-330.

[13] Kobayashi, M., Kakizono, T., Nagai, S., 1991. Astaxanthin production by a green-alga, *Haematococcus-pluvialis* accompanied with morphological-changes in acetate media. *J. Fermentation. Bioeng.*. 71, 335-339.

[14] Lemoine, Y., Schoefs, B., 2010. Secondary ketocarotenoid astaxanthin biosynthesis in algae: a multifunctional response to stress. *Photosynth. Res.*. 106, 155-177.

[15] Levitan, O., Dinamarca, J., Zelzion, E., Lun, D.S., Guerra, L.T., Kim, M.K., Kim, J., Van Mooy, B.A.S., Bhattacharya, D., Falkowski, P.G., 2015. Remodeling of intermediate metabolism in the diatom *Phaeodactylum tricornutum* under nitrogen stress. *P. Natl. Acad. Sci. USA.*. 112, 412-417.

[16] Li, Y., Sommerfeld, M., Chen, F., Hu, Q., 2008. Consumption of oxygen by astaxanthin biosynthesis: A protective mechanism against oxidative stress in *Haematococcus pluvialis* (*Chlorophyceae*). *J. Plant.*

ACCEPTED MANUSCRIPT

Physiol.., 165, 1783-1797.

[17] Li, Y., Sommerfeld, M., Chen, F., Hu, Q., 2010. Effect of photon flux densities on regulation of carotenogenesis and cell viability of *Haematococcus pluvialis* (*Chlorophyceae*). *J. Appl. Phycol.*. 22, 253-263.

[18] Melis, A., 2012. Photosynthesis-to-fuels: from sunlight to hydrogen, isoprene, and botryococcene production. *Energ. Environ. Sci.*. 5, 5531-5539.

[19] Miller, R., Wu, G., Deshpande, R.R., Vieler, A., Gaertner, K., Li, X., Moellering, E.R., Zaeuner, S., Cornish, A.J., Liu, B., Bullard, B., Sears, B.B., Kuo, M., Hegg, E.L., Shachar-Hill, Y., Shiu, S., Benning, C., 2010. Changes in Transcript Abundance in Chlamydomonas reinhardtii following Nitrogen Deprivation Predict Diversion of Metabolism. *Plant Physiol.*. 154, 1737-1752.

[20] Najafi, N., Hosseini, R., Ahmadi, A., 2013. The effect of gamma irradiation on astaxanthin synthetase encoding gene in two mutant strains of Phaffia rhodozyma. *Iranian J. Microbiology*.. 5, 293-8.

[21] Recht, L., Zarka, A., Boussiba, S., 2012. Patterns of carbohydrate and fatty acid changes under nitrogen starvation in the microalgae *Haematococcus pluvialis* and *Nannochloropsis sp. Appl. Microbiol. Biot.*. 94, 1495-1503.

[22] Rismani-Yazdi, H., Haznedaroglu, B.Z., Bibby, K., Peccia, J., 2011. Transcriptome sequencing and annotation of the microalgae *Dunaliella tertiolecta*: Pathway description and gene discovery for production of next-generation biofuels. *BMC Genomics*.. 12.

[23] Saakov, V.S., 2005. Pools of 14C-malic acid as a substrate for pyruvate production for the DOXP/MEP pathway of biosynthesis of carotenoids in chloroplasts. *Doklady. Biochemistry and biophysics*, 400, 7-13.

[24] Saha, S.K., McHugh, E., Hayes, J., Moane, S., Walsh, D., Murray, P., 2013. Effect of various stress-regulatory factors on biomass and lipid production in microalga *Haematococcus pluvialis*. *Bioresource Technol.*, 128, 118-124.

[25] Sanchez, J., Harwood, J.L., 2002. Biosynthesis of triacylglycerols and volatiles in olives. *Eur. J. Lipid. Sci. Tech.*. 104, 564-573.

[26] Shtaida, N., Khozin-Goldberg, I., Boussiba, S., 2015. The role of pyruvate hub enzymes in supplying carbon precursors for fatty acid synthesis in photosynthetic microalgae. *Photosynth. Res.*. 125, 407-422.

[27] Solovchenko, A.E., 2015. Recent breakthroughs in the biology of astaxanthin accumulation by microalgal cell. *Photosynth. Res.*.125, 437-449.

[28] Tang, D., Han, W., Li, P., Miao, X., Zhong, J., 2011. CO_2 biofixation and fatty acid composition of *Scenedesmus obliquus* and *Chlorella pyrenoidosa* in response to different CO_2 levels. *Bioresource Technol.*.102, 3071-3076.

[29] Wen, Z., Liu, Z., Hou, Y., Liu, C., Gao, F., Zheng, Y., Chen, F., 2015. Ethanol induced astaxanthin

ACCEPTED MANUSCRIPT

accumulation and transcriptional expression of carotenogenic genes in *Haematococcus pluvialis*. *Enzyme. Microb. Tech.*. 78, 10-17.

[30] Williams, P.J.L.B., Laurens, L.M.L., 2010. Microalgae as biodiesel & biomass feedstocks: Review & analysis of the biochemistry, energetics & economics. *Energ. Environ. Sci.*. 3, 554-590.

[31] Yuan, J., Peng, J., Yin, K., Wang, J., 2011. Potential health-promoting effects of astaxanthin: A high-value carotenoid mostly from microalgae. *Mol. Nutr. Food. Res.*.55, 150-165.

[32] Zheng, Q., Martin, G.J.O., Kentish, S.E., 2016. Energy efficient transfer of carbon dioxide from flue gases to microalgal systems. *Energ. Environ. Sci.*. 9, 1074-1082.

[33] Zhekisheva, M., Boussiba, S., Khozin-Goldberg, I., Zarka, A., Cohen, Z., 2002. Accumulation of oleic acid in Haematococcus pluvialis (Chlorophyceae) under nitrogen starvation or high light is correlated with that of astaxanthin esters. Journal of Phycology, 38, 325-331.

ACCEPTED MANUSCRIPT

ACCEPTED MANUSCRIPT

Fig. 1. Biomass dry weight and astaxanthin yield of *H. pluvialis* mutant red cells induced with 250 μmol photons m^{-2} s^{-1} light under 15% CO_2. (a) biomass dry weight, (b) astaxanthin yield.

Fig. 2. Transcriptome sequencing and annotation of *H. pluvialis* mutant red cells under 15% CO_2 and 250 μmol photons m^{-2} s^{-1} light. (a) volcano plot of mutant genes with significantly different expressions, (b) gene ontology (GO) classification of upregulated unigenes.

Fig. 3. Unigene transcript expression changes related to pyruvate metabolic pathways of *H. pluvialis* mutant red cells under 15% CO_2 and 250 μmol photons m^{-2} s^{-1} light (red genes: upregulate; green genes: downregulate; yellow genes: both upregulate and downregulate).

Fig. 4. Unigene transcript expression changes related to carotenoid biosynthesis pathways of *H. pluvialis* mutant red cells under 15% CO_2 and 250 μmol photons m^{-2} s^{-1} light (red genes: upregulate; green genes: downregulate).

Fig. 5. Unigene transcript expression changes related to fatty acid biosynthesis pathways of *H. pluvialis* mutant red cells under 15% CO_2 and 250 μmol photons m^{-2} s^{-1} light (red genes: upregulate; yellow genes: both upregulate and downregulate).

Table 1 Annotation and expression changes of significantly different unigenes related to pyruvate, carotenoid and fatty acid metabolic pathways.

ACCEPTED MANUSCRIPT

ACCEPTED MANUSCRIPT

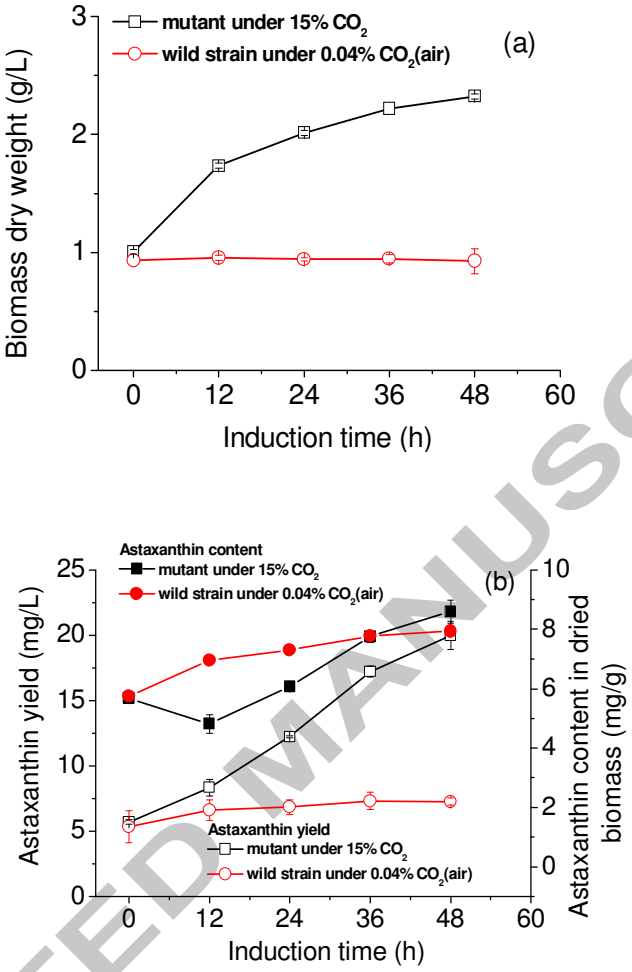

Fig. 1. Biomass dry weight and astaxanthin yield of *H. pluvialis* mutant red cells induced with 250 µmol photons m^{-2} s^{-1} light under 15% CO_2. (a) biomass dry weight, (b) astaxanthin yield.

ACCEPTED MANUSCRIPT

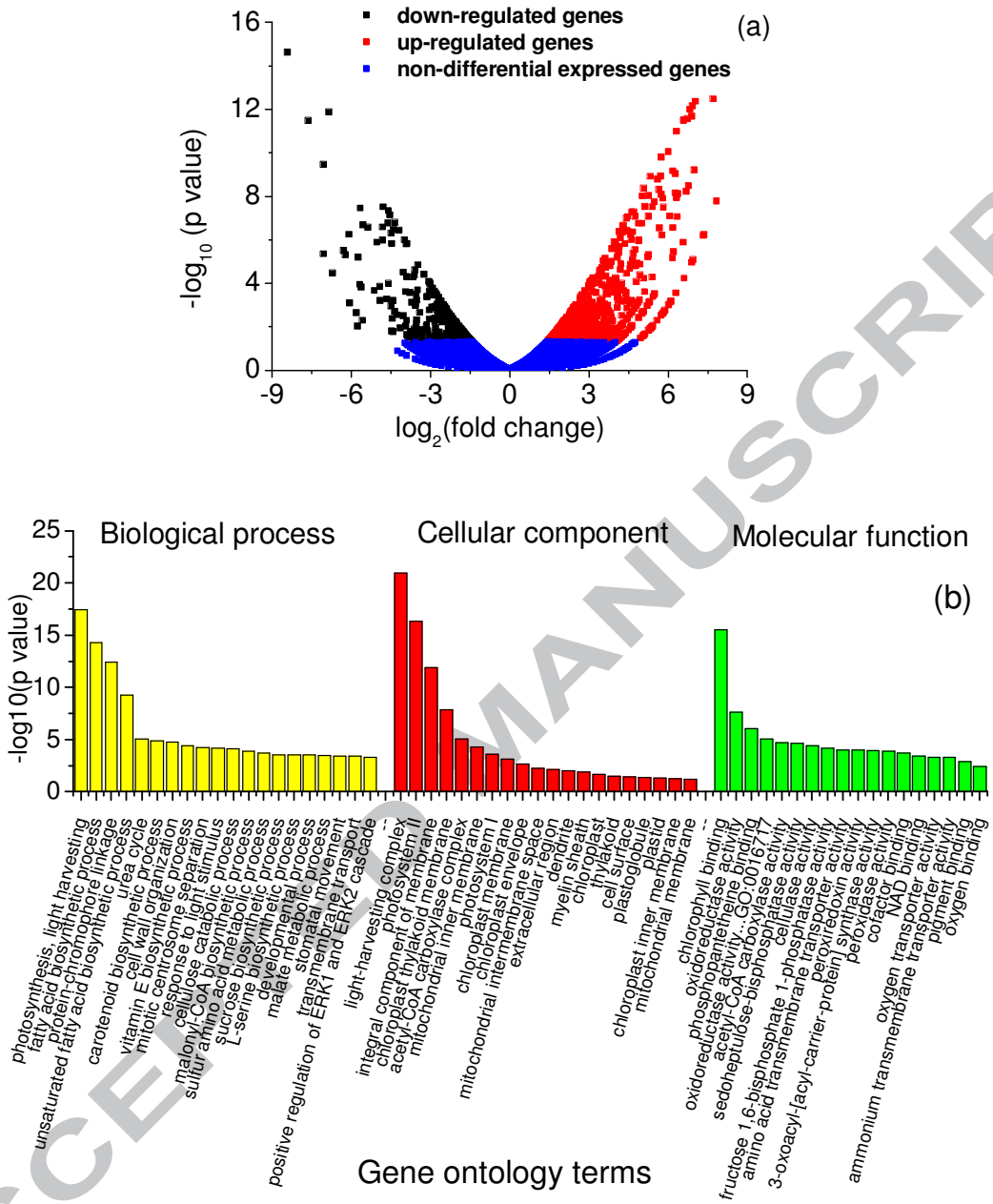

Fig. 2. Transcriptome sequencing and annotation of *H. pluvialis* mutant red cells under 15% CO_2 and 250 µmol photons m^{-2} s^{-1} light. (a) volcano plot of mutant genes with significantly different expressions, (b) gene ontology (GO) classification of upregulated unigenes.

ACCEPTED MANUSCRIPT

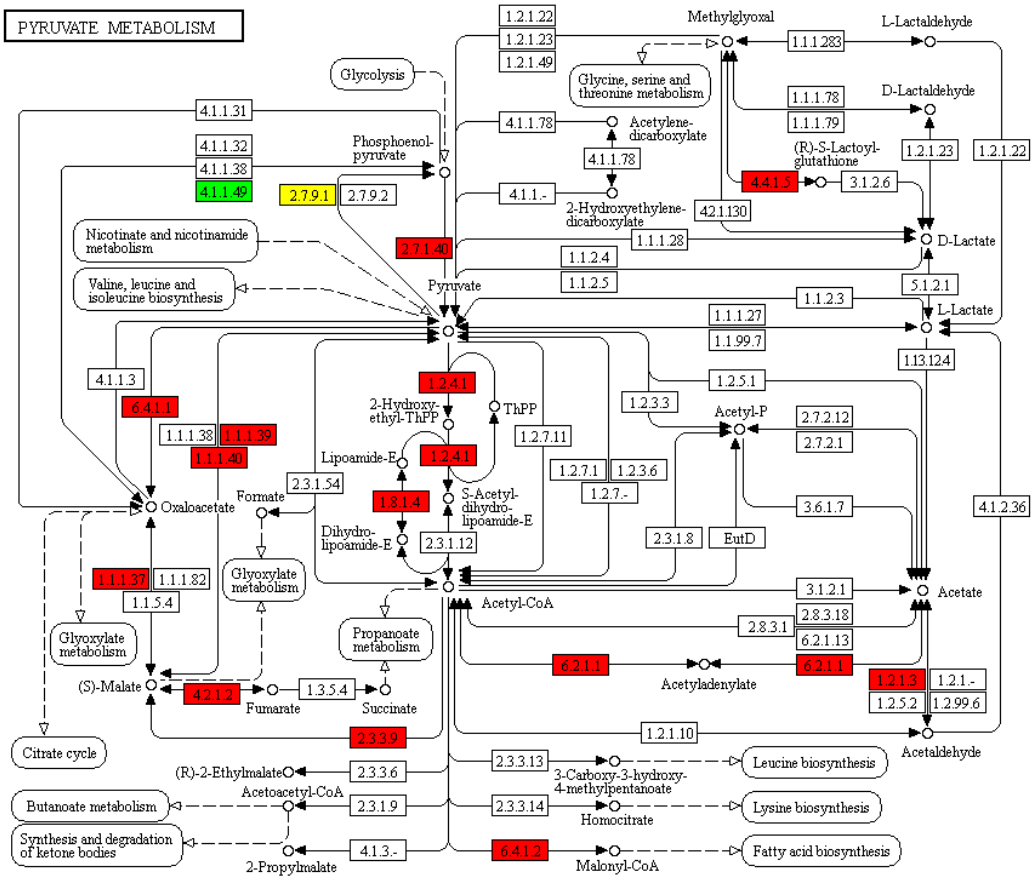

Fig. 3. Unigene transcript expression changes related to pyruvate metabolic pathways of *H. pluvialis* mutant red cells under 15% CO_2 and 250 μmol photons m^{-2} s^{-1} light (red genes: upregulate; green genes: downregulate; yellow genes: both upregulate and downregulate).

ACCEPTED

ACCEPTED MANUSCRIPT

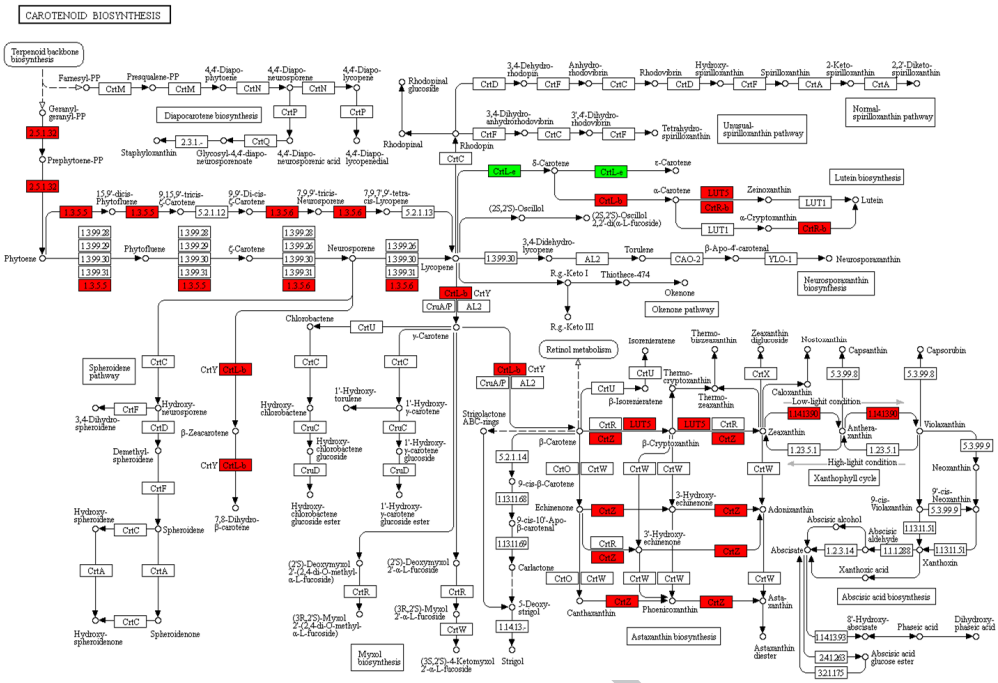

Fig. 4. Unigene transcript expression changes related to carotenoid biosynthesis pathways of *H. pluvialis* mutant red cells under 15% CO_2 and 250 μmol photons m^{-2} s^{-1} light (red genes: upregulate; green genes: downregulate).

ACCEPTED MANUSCRIPT

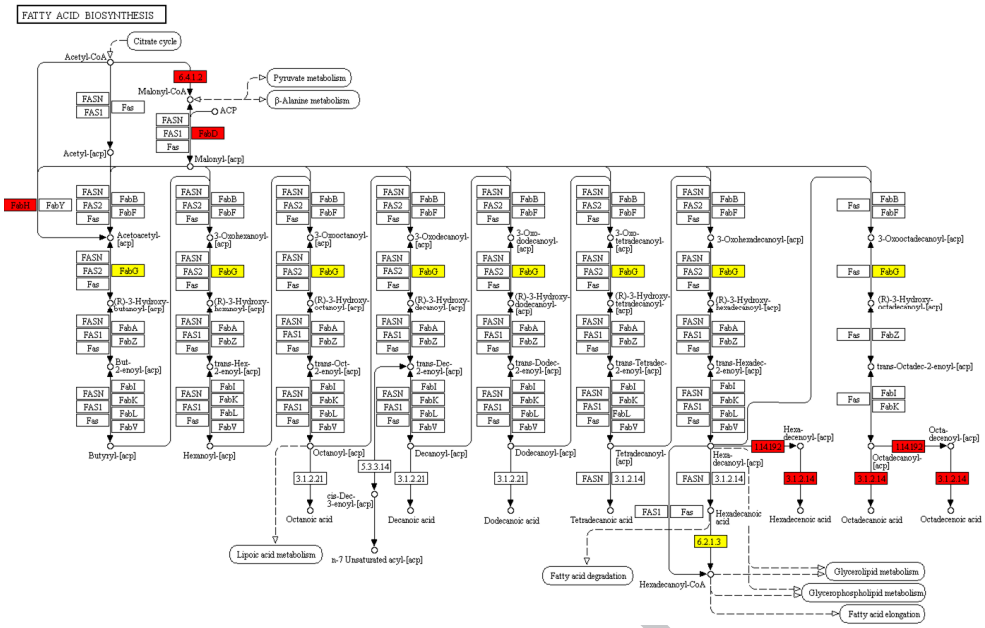

Fig. 5. Unigene transcript expression changes related to fatty acid biosynthesis pathways of *H. pluvialis* mutant red cells under 15% CO_2 and 250 µmol photons m^{-2} s^{-1} light (red genes: upregulate; yellow genes: both upregulate and downregulate).

ACCEPTED MANUSCRIPT

Table 1 Annotation and expression changes of significantly different unigenes related to pyruvate, carotenoid and fatty acid metabolic pathways.

EC No.	KO entry	KO name	KO definition	FC	-log10(p value)
KEGG term: Pyruvate metabolic pathway (KO00620)					
1.1.1.37	K00026	MDH2	malate dehydrogenase	3.47	1.31
1.1.1.39	K00028		malate dehydrogenase (decarboxylating)	Inf	1.48
1.1.1.40	K00029	NADP-ME	malate dehydrogenase (oxaloacetate-decarboxylating)(NADP+)	8.9	3.99
1.2.1.3	K00128		aldehyde dehydrogenase (NAD+)	Inf	1.66
1.2.4.1	K00162	PDHB	pyruvate dehydrogenase E1 component beta subunit	3.73	1.64
1.8.1.4	K00382	DLD	dihydrolipoamide dehydrogenase	4.93	1.95
2.3.3.9	K01638	aceB, glcB	malate synthase	3.71	1.71
2.7.1.40	K00873	PK	pyruvate kinase	3.54	1.83
2.7.9.1	K01006	ppdK	pyruvate, orthophosphate dikinase	2.71	1.31
4.1.1.49	K01610	pckA	phosphoenolpyruvate carboxykinase (ATP)	0.14	3.64
4.2.1.2	K01676	fumA, fumB	fumarate hydratase, class I	4.43	1.33
6.2.1.1	K01895	ACSS	acetyl-CoA synthetase	2.9	1.42
6.4.1.1	K01958	PC	pyruvate carboxylase	7.45	2.34
KEGG term: Carotenoid biosynthesis pathway (KO00906)					
1.3.5.5	K02293	PDS, crtP	15-cis-phytoene desaturase	3.19	1.34
1.3.5.6	K00514	ZDS, crtQ	zeta-carotene desaturase	4.41	2.17
2.5.1.32	K02291	crtB, PSY	phytoene synthase	10.43	4.01
CrtL-b	K06443	lcyB,	lycopene beta-cyclase	5.83	2.76
CrtZ	K15746	crtZ	beta-carotene 3-hydroxylase	18.39	4.61
LUT5	K15747	LUT5	beta-ring hydroxylase	5.3	1.81
KEGG term: Fatty acid metabolic pathway (KO00061)					
1.14.192	K03921	FAB2	acyl-[acyl-carrier-protein] desaturase	95.72	5.88
3.1.2.14	K10782	FATA	fatty acyl-ACP thioesterase A	8.33	4.06
6.2.1.3	K01897	ACSL	long-chain acyl-CoA synthetase	19	1.55
6.4.1.2	K01961	accC	acetyl-CoA carboxylase, biotin carboxylase subunit	2.95	1.32
	K01962	accA	acetyl-CoA carboxylase carboxyl transferase subunit alpha	3.62	1.69
	K01963	accD	acetyl-CoA carboxylase carboxyl transferase subunit beta	Inf	2.37
	K02160	accB, bccP	acetyl-CoA carboxylase biotin carboxyl carrier protein	3.08	1.32
FabD	K00645	fabD	[acyl-carrier-protein] S-malonyltransferase	6.74	3.35
FabG	K00059	fabG	3-oxoacyl-[acyl-carrier protein] reductase	35	1.67
FabH	K00648	fabH	3-oxoacyl-[acyl-carrier-protein] synthase III	3.13	1.57

ACCEPTED MANUSCRIPT

> Transcriptome sequencing and annotation was performed on *Haematococcus pluvialis*

> Astaxanthin metabolism of *H. pluvialis* was enhanced by gamma ray and 15% CO_2

> Pyruvate and fatty acid metabolism were enhanced to support astaxanthin biosynthesis

ACCEPTED MANUSCRIPT